THE JOURNAL OF PHYSICAL CHEMISTRY B

Article

pubs.acs.org/JPCB

Poly(AAc-*co*-MBA) Hydrogel Films: Adhesive and Mechanical Properties in Aqueous Medium

Dhamodaran Arunbabu, Hamed Shahsavan, Wei Zhang, and Boxin Zhao*

Department of Chemical Engineering and Waterloo Institute for Nanotechnology, University of Waterloo, 200 University Avenue West, Waterloo, Ontario, Canada N2L 3G1

ABSTRACT: Poly(acrylic acid-*co*-*N*,*N*′-methylenebisacrylamide) hydrogel films were synthesized by copolymerizing acrylic acid (AAc) with *N*,*N*′-methylenebisacrylamide (MBA) as a cross-linker via photo polymerization in the spacing confined between two glass plates. NMR spectroscopy was utilized to determine the cross-linking density. We found that the cross-linking density determined by NMR is higher than that expected from the feed concentrations of cross-linkers, suggesting that MBA is more reactive than AAc and the heterogeneous nature of the cross-linking. In addition to the swelling tests, indentation tests were performed on the hydrogel films under water to investigate effects of the cross-linking density on the adhesion and mechanical properties of the hydrogel films in terms of adhesive pull-off force and Hertz-type elastic modulus. As the cross-linker concentration increased, the effective elastic modulus of the hydrogel films increased dramatically at low cross-linking densities and reached a high steady-state value at higher cross-linking densities. The pull-off force decreased with increasing cross-linker concentration and reached a lower force plateau at high cross-linking densities. An optimal "trade-off" cross-linking density was determined to be 0.02 mol fraction of MBA in the hydrogel, where balanced elastic modulus and adhesive pull-off force can be obtained.

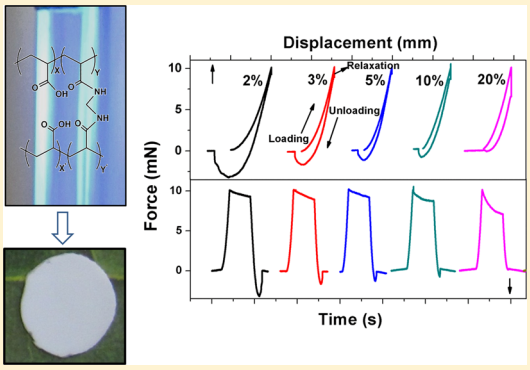

INTRODUCTION

Hydrogels are three-dimensional hydrophilic polymer networks holding a significant amount of water while maintaining their structural integrity without dissolution.[1,2] Hydrogels are ideal biocompatible materials used as skin, tissue, muco, and buccal adhesives in addition to popular applications in the fields of tissue engineering and drug delivery.[3−8] Hydrogel adhesion depends on both surface properties (e.g., surface charge density, dangling chains) and bulk mechanical properties. The elastic modulus of a loosely cross-linked hydrogel is close to that of typical pressure sensitive adhesives, whereas the elastic modulus of highly cross-linked hydrogels lies close to that of elastomers.[9] A hydrogel with effective adhesive properties must show a strong adhesion while maintaining mechanical integrity.[10] Characteristics of the hydrogels such as mechanical strength, degree of swelling, and adhesion depend upon their three-dimensional cross-linking density.[5,11] Finding an optimal cross-linking density where both strong adhesive and mechanical properties are met is crucial for developing hydrogel-based bioadhesives. Polyacrylic acid (PAA)-based hydrogels are typical bioadhesives used in drug delivery,[12] tissue engineering,[13] dermal patches,[4,14] biosensing material,[15] and hemodialysis.[16] Acrylic acid monomer can be readily cross-linked or copolymerized with functional monomers such as *N*-isopropylacrylamide[13] and 2-hydroxyethyl methacrylate or prepolymers such as poly(vinyl alcohol),[17] poly(ethylene glycol methacrylate),[18] or poly(ethylene glycol).[19] Much of the research has been conducted to investigate the polymer chemistry associated with hydrogels dealing with conjugation of hydrogels with drugs; the methodologies of synthesizing hydrogels from monomers, polymers, or existing hydrophilic polymers have been well developed. In contrast to the chemistry and bulk behavior of hydrogels, the physical or material aspects of hydrogel films are far less studied and less understood, partly because of the difficulties of fabricating uniform hydrogel films and complex biphasic behavior of hydrogels under geometrical confinement.

In this article, we report a novel way to fabricate poly(acrylic acid) (PAA) hydrogel films with controlled thickness and a systematic study of hydrogel films of varied cross-linking density and the effects of cross-linking density on the indentation behavior of hydrogel films. Poly(AAc-*co*-MBA) hydrogels were prepared using acrylic acid (AAc) as a monomer and *N*,*N*′-methylenebisacrylamide (MBA) as a cross-linker by UV assisted photopolymerization. MBA is the typical cross-linker for the preparation of PAA hydrogel by thermal polymerization. However, to the best of our knowledge, there is no report on the preparation of poly(AAc-*co*-MBA) hydrogel film by photopolymerization. Since MBA and acrylic acid are similar in their chemical structures, we hypothesized the poly(AAc-*co*-MBA) hydrogels may have a less chemical inhomogeneity and allow for a detailed study of

Received: October 15, 2012
Revised: November 22, 2012
Published: December 4, 2012

   dx.doi.org/10.1021/jp3101688 | *J. Phys. Chem. B* 2013, 117, 441−449

the relationship between cross-linking density and its adhesion and material behaviors. ^{1}H NMR spectroscopy was employed as an analytical tool to determine the cross-linking density. While the mechanical strength of the hydrogels has been studied using various methods such as tension, compression, shearing, and rheological measurements,[20−25] indentation-based tests were recently found more appropriate for characterizing mechanically weak hydrogels with heterogeneous surface or bulk properties,[26−33] particularly for hydrogel films. Axisymmetric indentation tests with a hemispherical elastomer probe were implemented in this study to characterize the mechanical and adhesive properties of the synthesized hydrogels in the framework of contact mechanics. The relationship between cross-linking density and indentation characteristics was established. Furthermore, an optimal "trade-off" cross-linking density was determined, where the balanced elastic modulus and adhesive pull-off force can be obtained.

EXPERIMENTAL METHODS

Synthesis of Poly(AAc-*co*-MBA) Hydrogels. The poly(AAc-*co*-MBA) thin film hydrogels were synthesized by photopolymerization in the spacing confined between two parallel glass plates. Acrylic acid (Fisher Scientific), *N*,*N*-methylenebisacrylamide (Sigma-Aldrich), and photoinitiator 2,2′-dimethoxyacetophenone (Sigma-Aldrich), DMSO (Sigma-Aldrich), and D_2O (Cambridge Isotope Laboratories Inc.) were used as received. A 0.300 g portion of acrylic acid was added dropwise to a glass vial containing *N*,*N*′-methylenebisacrylamide with different concentrations, and then 2 g of deionized water was added. This monomer solution was mixed by vortex to obtain a homogeneous mixture. A 40 μL portion of 2,2′-dimethoxyacetophenone or DEAP (10% (V/V) solution in DMSO) was added to the monomer solution and mixed. The monomer solution was injected into the spacing between two glass slides separated by a parafilm film (thickness ≈ 720 μm) spacer with hollow rectangular interior, as shown in Figure 1. The injected monomer solution

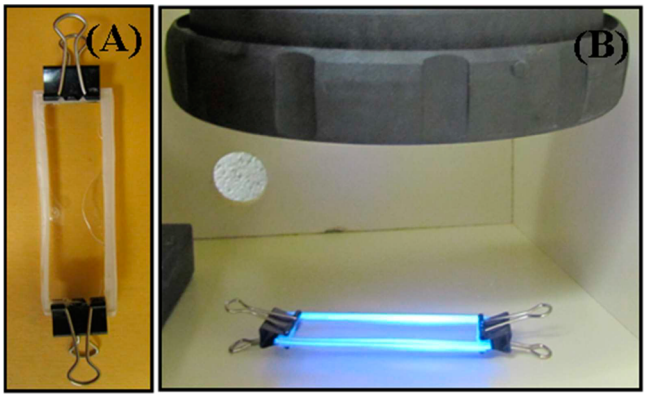

Figure 1. (A) The microscopic slide vessel and (B) experimental setup used for the polymerization of hydrogel thin films.

was placed 10 cm below a UV lamp (Built-in-ballast UV lamp, 365 nm, Hg source, Sigma-Aldrich) for 4 h to be photopolymerized as a thin hydrogel film. After that, the two glass slides were separated gently; the hydrogel film adhering to any one of the glass slides was washed extensively with Milli-Q water to remove unreacted monomers/initiator if any. The resultant hydrogel films were stored in Milli-Q water. Thin film poly(AAc-*co*-MBA) hydrogels with various MBA concentrations were synthesized. The concentration of the cross-linker varied from 2 to 30% (relative weight percentage to that of AAc). Except the cross-linker concentration, all other parameters including polymerization time, concentration of the initiator, water, and principal monomer (AAc) were kept constant. Scheme 1 depicts the photopolymerization pathway of poly(AAc-*co*-MBA) hydrogel.

H^1 NMR Spectroscopy. NMR spectroscopy was used as an analytical tool to determine the degree of cross-linking or the cross-linking density of the P(AAc-*co*-MBA) hydrogel. For the NMR analysis, hydrogel reaction mixtures were prepared with different MBA concentrations of 2, 3, 4, 5, 8, 10, 20, and 30% (relative to the acrylic acid weight) maintaining other parameters constant as explained in the previous section. Polymerization was carried out in deuterium oxide (D_2O) instead of water. Measured volumes of polymerization mixtures were injected in NMR tubes slowly to avoid the formation of air bubbles. The polymerizations were carried out inside NMR tubes under a UV lamp (365 nm, Hg source) for 4 h. NMR spectroscopy was performed on two different sets of poly(AAc-*co*-MBA) hydrogels prepared under the same photopolymerization conditions for both kinetics and cross-linker concentration variation studies.

To check if there were any unreacted materials in the NMR tubes, we performed an additional set of experiments to completely wash the hydrogels before NMR tests. For doing these, after the completion of the polymerization, hydrogels were removed out of the NMR tubes and immersed in D_2O for 48 h to remove unreacted monomers and initiators. During the cleaning process, D_2O was replaced with a fresh stock after 24 h. NMR measurements consisting of 16 scans were performed on all three sets of hydrogels in a 300 MHz Bruker NMR instrument (Bruker-AVANCE-DPX-300). The NMR spectra obtained were analyzed using MestReNova software (Version 7.1.1., MestReLab Research). Relative peak intensities, obtained by keeping the aliphatic methyne (−CH) signal as a base and integrating all the peaks, were used to estimate the cross-linking density. Time dependent NMR studies were also conducted on poly(AAc-*co*-MBA) hydrogels with 2% feed cross-linkers to investigate the decay of monomer peaks and the growth of polymer peaks. Six NMR tubes containing the polymerization mixture were prepared in a similar fashion as described above and were polymerized under the UV lamp. Each NMR tube was exposed to UV light for different times—5, 10, 15, 20, and 30 min—and stored in a dark container for a while before recording the NMR spectroscopy.

Swelling Experiment. Swelling tests were performed to determine the degree of swelling of the synthesized hydrogel films. Hydrogels of different cross-linker concentrations were separated from glass slides; all the hydrogel films were retained in Milli-Q water of fixed pH 6.8 for 24 h. After 24 h, the gels have reached their maximum swollen state; circular disks of the hydrogel were cut and blotted with weighing paper to remove surface free water. Blotted hydrogels were then weighed and air-dried inside a Petri dish for 24 h. The degree of the swelling of the hydrogel, *S*, is calculated from the following equation:

$$S = \frac{W - W_0}{W_0} \times 100 \quad (1)$$

where W and W_0 stand for the weight of the swollen hydrogel and the weight of the dried hydrogel, respectively.

dx.doi.org/10.1021/jp3101688 | J. Phys. Chem. B 2013, 117, 441−449

Scheme 1. Schematic Representation of the Photopolymerization of Poly(AAc-*co*-MBA) Hydrogels

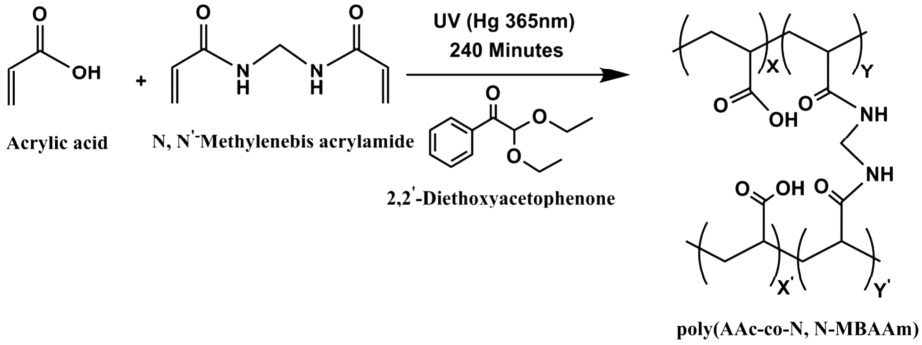

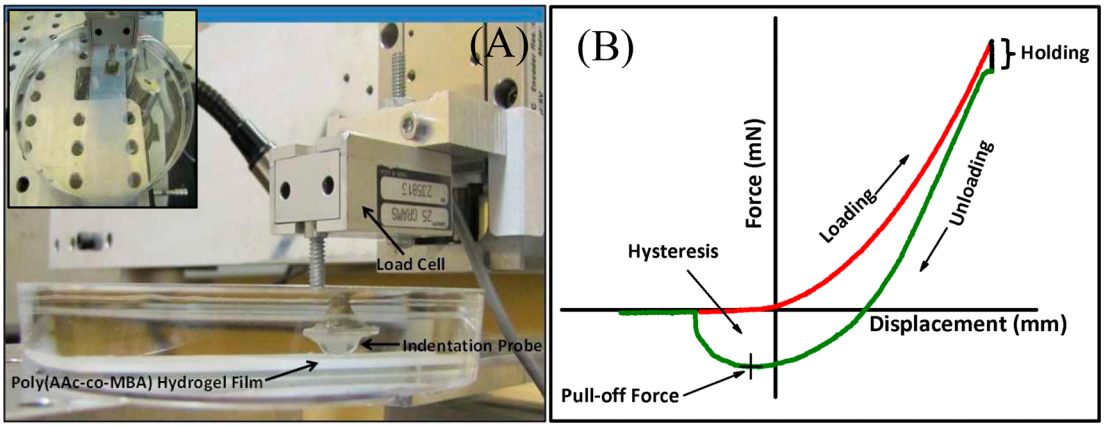

Figure 2. (A) Experimental setup of the underwater indentation experiments on poly(AAc-*co*- MBA) hydrogel films. (Inset: Top view of the setup.) (B) A typical force vs displacement curve obtained during the indentation of poly(AAc-*co*-MBA) hydrogels.

Indentation of Hydrogels. Adhesive and mechanical properties of the hydrogel samples were characterized by indenting a 6 mm diameter hemispherical elastomer probe using a custom-made indentation apparatus equipped with a 0–25 g load cell (GSO-25, Transducer Techniques) and bottom-view microscope, as shown in Figure 2. Probes used in this study were made of fully cured polydimethylsiloxane (PDMS). First, a 10:1 wt ratio of Sylgard 184 monomer and cross-linker (Dow Chemical Company) was casted in a hemispherical negative Teflon master-mold and then cured at 90 °C for 1 h. Second, a thin layer of PDMS mixture was manually poured on the molded hemisphere to form a nearly smooth shell and then cured at 90 °C for 1 h. The probes were glued to a 4 cm shaft and mounted on the load cell to facilitate the indentation tests under fully immersed conditions. The hydrogel film samples were fixed on the glass slides, attached to the bottom of the Petri dishes, and fully immersed in Millipore DI water. Indentation tests were performed with a constant velocity of 1 μm/s with a holding time of 240 s between loading and unloading periods. Load–displacement data were recorded and used to extract the characteristic parameters for the adhesive and mechanical properties of the hydrogel samples. Each experiment was repeated at least 6 times; the mean value and standard deviation were reported.

RESULTS AND DISCUSSION

PAA Hydrogel Thin Films and Their Degree of Swelling. Different from the bulk hydrogels, we found hydrogel films are difficult to handle because they are fragile and easy to dehydrate. In this study, we developed an alternative technique modified from the previously reported methods[15,34] to fabricate hydrogel films with controlled thickness between two parallel glass slides. One glass slide was utilized for carrying the hydrogel films, in a way similar to the construction of pressure sensitive adhesive tape with a backing material. The other glass slide was used to control the thickness of hydrogel films. The top glass slide is transparent, allowing the UV light to penetrate into the reaction solutions and the transparent bottom slide let the unutilized light source to exit. This setup also prevents the evaporation of water caused by the heat emitted by the UV lamp during the synthesis process.

PAA hydrogel thin films were synthesized with varied cross-linker concentrations in the reaction mixture or the feed. As expected, the hydrogel with a low cross-linker concentration was transparent; it became opaque as the cross-linker concentration in the feed solution increased, indicating the formation of a denser polymer network in the gel which scatters more light. To evaluate the cross-linking density of the gel quantitatively, we first performed the swelling tests at the macroscopic scales. When the gel is in contact with an aqueous solution, the network swells due to the thermodynamic compatibility of the polymer chains and water. Since the carboxylic groups inside the hydrogel are ionized at the neutral pH, the concentration of the counterion inside the hydrogel film is higher than that in the bulk water, creating a potential energy gradient known as Donnan membrane potential across the hydrogel/water interface.[34–37] This Donnan membrane potential leads to an osmotic pressure inside the hydrogel pores. Thus, there are two driving forces for the swelling of the

dx.doi.org/10.1021/jp3101688 | J. Phys. Chem. B 2013, 117, 441–449

PAA gel: the free energy of mixing of polymer chains with solvent medium (ΔG_{mix}) and the free energy of ionic electrostatic energy resulting from Donnan membrane potential and electrostatic repulsion between charged ionic groups of the polymer backbone (ΔG_{ionic}). These swelling forces are counterbalanced by the retractive force induced by the cross-links of the network or the free energy of elasticity of cross-linked networks ($\Delta G_{elastic}$). Swelling equilibrium is reached when the summation of these free energy contributions[35] is $\Delta G_{total} = \Delta G_{mix} + \Delta G_{ionic} + \Delta G_{elastic} = 0$. For PAAc hydrogels of different cross-linker concentration at neutral pH, they can reach equilibrium swelling state in 8 h.[5] In our cases, all the hydrogel films were soaked in water for 24 h; thus, the gels reached their maximum swollen state.

Generally, the cross-linker concentration is directly related to the resultant cross-linking density of the gel. At lower cross-linker concentration, the gel has lower cross-linking density and hence higher swelling capacity, whereas the gel formed with higher cross-linker concentration will have higher cross-linking density, lowering the swelling capacity. Furthermore, when the cross-linking density increases, the pore size inside hydrogel films decreases, bringing more carboxylic acid groups of monomers to form hydrogen bonds; this situation reduces the degree of ionization of the carboxyl groups or the amount of free carboxylate ion (COO^-) sites. Figure 3 shows the

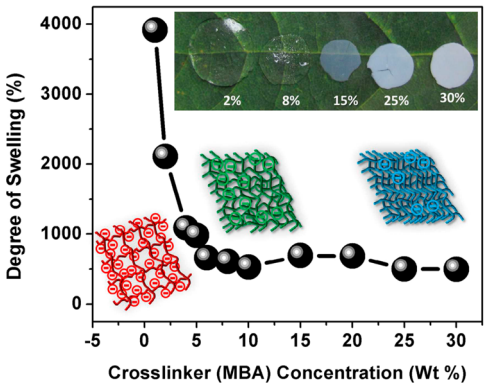

Figure 3. Degree of swelling as a function of the cross-linker *N*,*N*′-methylenebisacrylamide (MBA) concentration. (Inset: Images of hydrogels of different cross-linker concentration; transparent to opaque transformation.)

degree of swelling as a function of the feed concentration of the cross-linker MBA. As the feed cross-linker concentration C_{feed} increased, the degree of swelling rapidly decreased from 4000 to 500% when C_{feed} < 10 wt % (relative to the acrylic acid) because of the reduced pore size and decreased ionization or acid dissociation constant (pK_a) of carboxylic acid groups. It is interesting to note that the degree of swelling became constant when C_{feed} > 10 wt %, suggesting the feed cross-linker might be more than sufficient. However, the increase of opaqueness of the hydrogel films indicated a denser hydrogel network or higher degree of cross-links creating more pores but having smaller pore sizes. Thus, more cross-links formed as the feed concentration increased even when C_{feed} > 10 wt %. The increased cross-links should have further made the degree of swelling decrease, but we observed a constant degree of swelling for C_{feed} > 10 wt %. We suspect that the acid dissociation constant (pK_a) of the carboxylic groups of PAA might have reached a minimum value at C_{feed} ~ 10 wt % because high cross-linking density restricted the diffusion of protons in the network; the further increase in cross-links would not be able to reduce the osmotic driving force any more. Therefore, neither the feed cross-linker concentration nor the degree of swelling is directly related to the real cross-link density. In the following section, we employed the NMR technique to investigate the nature of cross-linking and estimate the compositions of the hydrogels.

NMR Analysis of Poly(AAc-*co*-MBA) Hydrogel Composition. As illustrated in Scheme 1, the synthesis reaction of the poly(AAc-*co*-MBA) hydrogel is a copolymerization of AAc and MBA where the divinyl groups of MBA cross-link neighboring polymer chains. It is reported that hydrogels synthesized from acrylamide (CH_2═CH—CO—NH_2) and MBA have different reactivity ratios.[40] AAc (CH_2═CH—COOH) is structurally similar to acrylamide and MBA. Thus, heterogeneous copolymerization is expected. NMR spectroscopy has been found in the literature as an effective tool to estimate the compositions of many types of copolymers.[38,39] The NMR spectra are a representative of copolymer chains of equal degree of polymerization which forms the majority of the total number of chains.[41,42]

To the best knowledge of the authors, there is no report of the detailed NMR analysis of poly(AAc-*co*-MBA) hydrogel. A similar NMR spectroscopy assisted study was reported recently to estimate the reactivity ratio of an acrylamide and *N*,*N*′-methylenebisacrylamide hydrogel system in which thermal initiation was employed.[40] We intended to estimate the molar fractions of monomer A (f_1) and monomer B (f_2) present in the copolymer backbone and then the cross-linking density of the hydrogels. For this, we first investigated the polymerization of monomers with respect to time by analyzing the growth and decay of chemical shifts of the NMR spectra of the reaction mixtures, from which the chemical shifts characteristic of the poly(AAc-*co*-MBA) hydrogel were identified. Second, the variation in the intensity of the characteristic chemical shifts with respect to the feed cross-linker concentrations was investigated and used to determine the degree of cross-linking of the hydrogels.

Figure 4 shows typical NMR spectra of polymerization mixtures with a 2% cross-linker feed concentration exposed under UV irradiation for different time periods (t = 0, 5, 10, 15, 20, and 30 min). The chemical structures of acrylic acid (AAc) and *N*,*N*′-methylenebisacrylamide (MBA) are shown at the left and middle top, and the structure of the poly(AAc-*co*-MBA) was shown at the right top. The protons in these chemical structures and their corresponding H^1 NMR signals are denoted as A for −CH− at the chemical shift δ = 2−2.5, B for $-CH_2$ at δ = 0.8−2 in the poly(acrylic acid) backbone structure, C for −NH at δ = 7.8, and D for $-CH_2-$ groups linked to two −NH groups of MBA at δ = 4.6 ppm. The vinyl protons of monomers are designated as E at δ = 5.8 ppm, F at δ = 6.0 ppm, and G at δ = 6.2 ppm. In addition, the peak at 2.7 ppm corresponds to deuterated DMSO and a peak at 4.7 ppm corresponds to deuteron exchanged residual water (HOD) in the NMR solvent (D_2O).[40,41] Note that the signal for the carboxylic proton of acrylic acid is expected at δ = 11 but is absent in the spectra because these protons were deuterated by D_2O. The signals corresponding to the amide proton −NH of MBA monomer occur at δ = 7.8 ppm but are weak because of the partial deuteration. The growth and decay of these NMR peaks with respect to time during the polymerization provided information about the rate of monomer conversion and cross-

dx.doi.org/10.1021/jp3101688 | J. Phys. Chem. B 2013, 117, 441−449

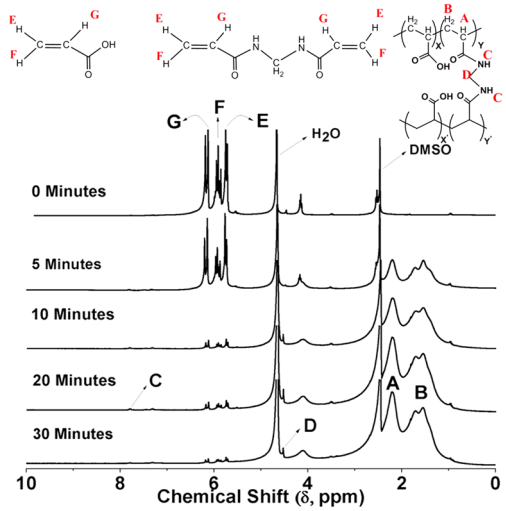

Figure 4. H^1 NMR spectra of 2% poly(AAc-*co*-MBA) hydrogel recorded at different time intervals. Given spectra illustrate photopolymerization kinetics of 2% poly(AAc-*co*-MBA) hydrogel. Peaks were designated with respective protons in the polymer backbone.

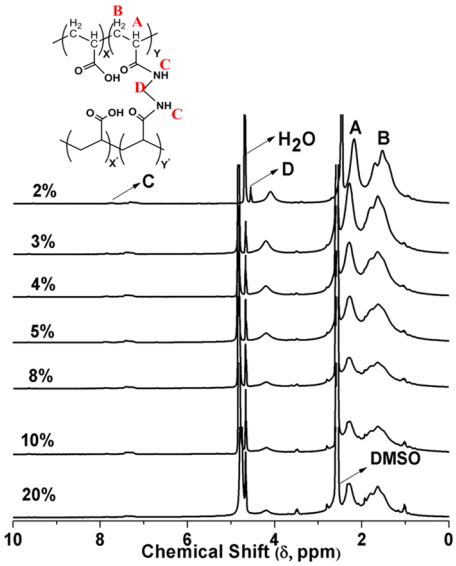

Figure 5. H^1 NMR spectra of poly(AAc-*co*-MBA) hydrogels with different feed MBA concentrations.

linking kinetics. Examination of the NMR spectra revealed that the intensities of the vinyl protons E, F, and G (5.8−6.5) of the monomers decrease rapidly while the intensities of alkyl protons (−CH_2, peak A at 2.2−2.5 ppm and −CH peak B at 0.8−2 ppm) increased rapidly. The rapid disappearance of vinyl peaks and sudden growth of methyl peaks (δ = 0.8−2.5 ppm) suggest that the majority of acrylic acids were converted into polymers within 10 min. Furthermore, the intensity of methylene proton signals of MBA (H_D, at 4.6 ppm) increased with time, indicating the insertion or cross-linking of MBA in the polymer backbone. The relative peak intensity of H_D increased slowly, which is possibly due to the lower concentration of MBA (2%) compared with acrylic acid concentration (100%) whose polymerization appears quickly. Overall, the analysis of time-dependent NMR measurement revealed that the polymerization process was rapid. To ensure the complete conversion of monomers, we exposed all the polymerization mixtures to UV irradiation for 4 h as described elsewhere[15,34] and studied the degree of cross-links at varied feed concentrations of MBA.

Figure 5 shows typical NMR spectra of poly(AAc-*co*-MBA) hydrogels with different MBA concentrations. The three sets of hydrogels (washed and unwashed) synthesized in the NMR tubes showed the same NMR spectra, suggesting that all monomers were polymerized and no unreached species were in the NMR tubes. It was confirmed by the absence of vinyl protons E, F, and G (5.8−6.5) of the monomers in all the spectra. The complete conversion is also evidenced by the constant intensity of alkyl protons (peaks A and B) that is the summation of alkyl proton signals of AAc and MBA. Because AAc and MBA are in similar chemical environments and resonate at similar magnetic frequency or show peaks at similar chemical shifts, it is impossible to differentiate the contributions from AAc or MBA to the A and B due to their subtle difference in the chemical environments. Thus, the insertion of MBA into the polymer backbone has a negligible influence on the intensities of peaks A and B. In contrast, the intensities of peak D increase with the increase in MBA concentration in the feed solution because of the formation of cross-linking between the polymer backbones. On the basis of this observation, we proposed to estimate the mol fraction of the MBA or the density of cross-linking from the measured peak intensities of protons A, B, and D. Note that the determined mol fraction of the MBA of the hydrogels would represent the majority of copolymer chains of similar degree of polymerization, which may be different from that of the feed reactants.

To obtain quantitative information, we use X to represent the number of AAc repeating unit moieties and Y to represent the number of MBA repeating unit moieties in the backbone. The mol fraction of AAc is $f_1 = X/(X + Y)$, and the mol fraction of MBA is $f_2 = Y/(X + Y)$. Hence, the degree of cross-linking of the hydrogel is f_2. The intensity of peak A, I_A, is proportional to the number of H_A protons (−CH), whereas the intensity of peak B, I_B, is proportional to the number of H_B protons (−CH_2); both of them are directly proportional to $(X + Y)$, which is a constant. Furthermore, it can be seen from Figure 5 that the area of peak A is almost half of the peak area of peak B, reflecting the fixed ratio between H_A and H_B in the polymer backbone. Thus, we can arbitrarily assign $I_A = 1$ and use it as a base to evaluate the variation of peak D that corresponds to the amount of MBA in the copolymer or the degree of cross-linking. If the polymer chain is fully cross-linked or is a homopolymer of MBA, it can be expected that two D protons should give a peak with a similar intensity I_D to that of peak B (I_B). It was observed that I_D increases with the feed concentration of cross-links but always less than I_B. Numerical values of peak intensities of A, B, and D protons extracted from Figure 5 were tabulated in Table 1. For a finite density of cross-linking, we have

$$f_2 = \frac{Y}{X + Y} = \frac{I_D}{I_B} \quad (2)$$

The average concentrations of AAc (f_1) and MBA (f_2) in a copolymer hydrogel chain were obtained by substituting the peak intensities estimated from three sets of NMR spectra in eq 2. Table 2 summarizes the average concentrations of AAc (f_1) and MBA (f_2) along with the theoretical values (F_1 and F_2) expected from the feed compositions. Figure 6 plots the average mol fraction values of MBA (f_2) in the copolymer against the mol fraction of MBA (F_2) in the feed. The dotted straight line

dx.doi.org/10.1021/jp3101688 | J. Phys. Chem. B 2013, 117, 441−449

Table 1. Integral Values of Peak Intensities Estimated from NMR Spectra Given in Figure 5[a]

%	I_A	I_B	I_D	Y
2	1	1.83	0.03	0.016
3	1	1.67	0.06	0.036
4	1	1.77	0.07	0.040
5	1	1.83	0.09	0.049
8	1	1.96	0.17	0.087
10	1	1.75	0.2	0.114
20	1	1.74	0.32	0.184

[a]Peak A is taken as a reference ($I_A = 1$), and the rest of the peaks were integrated. Y is the mol fraction of MBA unit in poly(AAc-*co*-MBA) hydrogels.

Table 2. AAc and MBA Concentration in the Feed and in the Copolymer, Average Degree of Cross-Linking (f_2), and Percentage Cross-Linking (P) Values as Estimated from NMR Spectra Performed on Three Different Sets of Poly(AAc-*co*-MBA) Hydrogels Prepared under Identical Conditions

MBA (%)	F_1(AAc) Theo	f_1(AAc) Exp, X	F_2(MBA) Theo	f_2(MBA) Exp, Y	$P = 100Y$ (%)
2	0.991	0.989	0.009	0.011	1.12
3	0.986	0.980	0.014	0.020	2.00
4	0.982	0.968	0.018	0.032	3.20
5	0.977	0.954	0.023	0.046	4.60
8	0.964	0.898	0.036	0.102	10.2
10	0.955	0.877	0.045	0.123	12.3
20	0.915	0.824	0.085	0.176	17.6

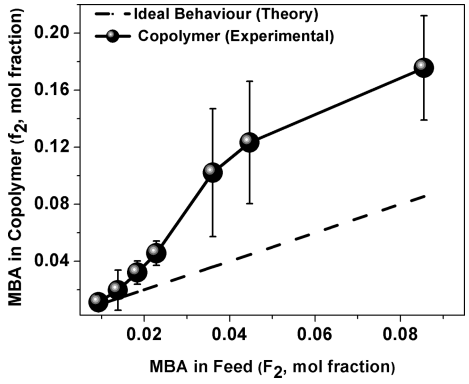

Figure 6. A plot of cross-linker concentration in the copolymer against concentration of cross-linker in the feed.

represents the ideal behavior where the input amount of cross-linker in the feed (F_2) is equal to the output in the copolymer (f_2) backbone. At low molar fractions, $F_2 < 0.015$, f_2 is almost the same as F_2 in the feed. At higher molar fractions, f_2 is significantly larger than F_2, suggesting that the resultant degree of cross-linking obtained from the NMR analysis is more than expected from feed. For copolymerization, the reactivity ratio of the monomers determines the relative amount of the monomers in the polymer backbone. The observation of $f_2 > F_2$ may indicate that MBA is more reactive and easier to be inserted into the polymer backbone when $F_2 > 0.015$. Thus, the yielded hydrogel would have heterogeneity in its surface and the bulk, which affects its physical and chemical characteristics. This heterogeneous copolymerization might have led to the formation of random bulk polymer domains in the polymer backbone and consequently influence the mechanical and adhesive properties of hydrogel films.

Indentation Behaviors of Thin Film Hydrogels and the Effects of Cross-Linking Density. To investigate the effect of cross-linking density on the mechanical and adhesion properties of poly(AAc-*co*-MBA) hydrogel films, we carried out a series of microindentation tests. In comparison to the commonly used tension, compression, shearing, and rheological tests to characterize the bulk properties, indentation based tests are more appropriate for handling mechanically weak hydrogels with heterogeneous surface or bulk properties.[19−26] Furthermore, we have incorporated the features of the axisymmetric adhesive tests to the indentation test so that we can determine the interfacial interactions and the local bulk mechanical properties simultaneously. The challenge for the characterization of the fully hydrated polymers was overcome by performing the tests with a long shaft in fully immersed conditions.[43,44] There is always a certain amount of repulsive/attractive hydrodynamic forces during the approaching/retracting of mating surfaces in a liquid medium.[45] The hydrodynamic effects were small in our indentation tests because a relatively high preload was applied to cause a large deformation of the hydrogels; this type of indentation studies allowed us to investigate the material properties of the hydrogels. In addition to the adhesive force, the local hardness and reduced elastic modulus of the samples can be calculated by analyzing the loading−unloading curves, as illustrated in Figure 2B, according to well-established contact mechanics equations.[27]

Figure 7A−F shows typical force vs displacement curves for the indentation tests on the samples synthesized with different

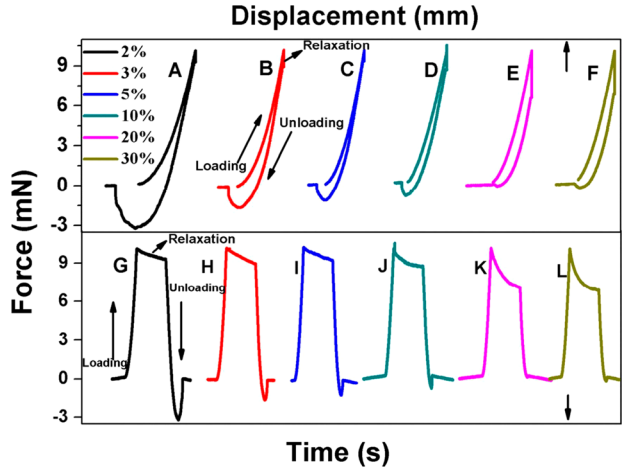

Figure 7. Plots of force as a function of displacement (top) and time (bottom) for poly(AAc-*co*-MBA) hydrogels of different cross-linker concentrations.

concentrations of the cross-linker MBA ranging from 2 to 30%. It is obvious that the indentation curves changed dramatically as the concentration increased: the pull-off force and loading−unloading hysteresis decreased with increasing amount of cross-linkers. Figure 7G−L shows the force vs time curves to have a better view of the relaxation behavior of the hydrogel samples. Different behaviors of the force relaxation were observed for the samples of different cross-linking contents. Detailed characterization of hydrogels' mechanical and adhesive properties is challenging because hydrogels are biphasic and have

dx.doi.org/10.1021/jp3101688 | J. Phys. Chem. B 2013, 117, 441−449

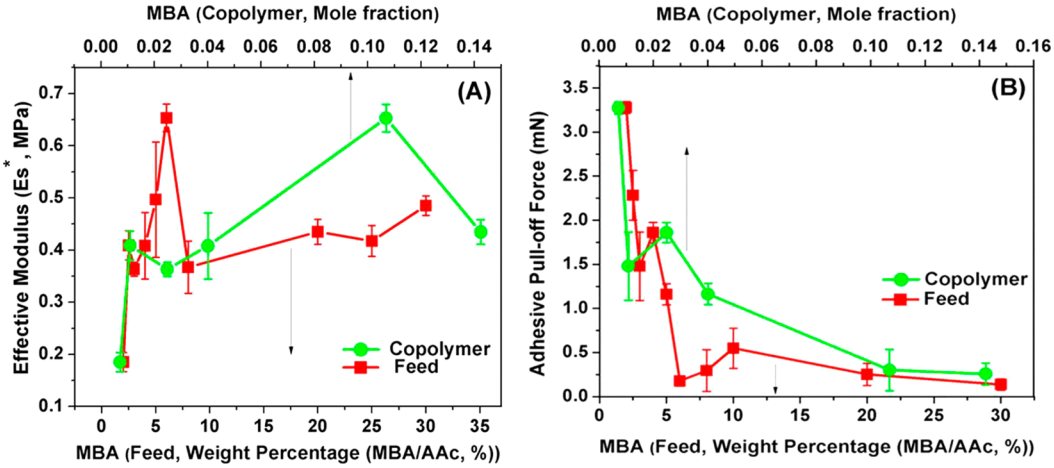

Figure 8. (A) Plots of elastic modulus of the hydrogel films as functions of the feed MBA concentration and the NMR-determined mol fraction of MBA in the hydrogel. (B) Plots of adhesive pull-off forces of the hydrogel films as functions of the feed MBA concentration and the NMR-determined mol fraction of MBA in the hydrogel.

pronounced time-dependent behaviors.[46] In fact, the most readily observed time-dependent behavior of hydrogels is the creep or the stress relaxation in a constant loading period.[40] Although the relaxation behavior is interesting and able to provide fundamental insights on the viscoelastic and poroelastic deformations, this study focused on the quantitative information obtained directly from the indentation curves. The pull-off force during separation is a characteristic parameter for the adhesion interaction between the hydrogel film and the PDMS probe; we used it to evaluate the effect of cross-linking density on the adhesive properties of hydrogel film. The pull-off process took place gradually instead of a sudden snap off the probe. We attribute this behavior to a gradual peeling of the hydrogel from the PDMS probe.

We further analyzed the loading branch of indentation curves in the framework of contact mechanics to obtain a characteristic parameter for the bulk mechanical properties. For this, we first estimated the level of strain induced in the indentation test; they ranged from 0.08 to 0.11; i.e., for a fixed preload of 1 g, using a Sylgard 184 hemispherical tip, the absolute indentation depth ranged from 50 to 80 μm. Thus, to a first order of approximation, we assumed linear elastic behaviors in the loading and neglected the adhesion between the PDMS probe and hydrogel films because of the weakening effect of water and the short contact time. On the basis of these assumptions, the classical Hertz contact theory is applied, which relates the loading force F to the displacement d by the following equation.

$$F = \frac{4}{3}E^*R^{1/2}d^{3/2} \tag{3}$$

where R is the radius of the indenter (3 mm) and E^* is a combined or reduced Young's modulus of the tip and sample. E^* was determined by fitting of the data points obtained from loading branch of the force vs displacement curves. E^* is related to Young's modulus and Poisson's ratio of the indenter tip E_t, ν_t and the sample E_s, ν_s by eq 4.

$$\frac{1}{E^*} = \frac{1-\nu_t^2}{E_t} + \frac{1-\nu_s^2}{E_s} \tag{4}$$

The tip used in our experiments is made of PDMS Sylgard 184, a well-known silicone rubber with a known Poisson's ratio of 0.5. The Young's modulus of the tip was determined by its indentation on a rigid glass substrate to be 1.8 MPa. In this way, we obtained the reduced Young's modulus of the hydrogel samples ($E_S^* = E_S/(1-\nu_s^2)$), even if we do not know the exact value of the Poisson's ratio. Note the JKR theory might be applied to obtain more insights on the interfacial energy if the area of the contact spot can be measured, but we were not able to measure the contact area due to the opacity of the hydrogels and also the limitation of our instrument.

Figure 8 plots these two characteristic parameters of the indentation curves (the adhesive pull-off force and the reduced elastic modulus of the hydrogel films) as functions of the concentration of added cross-linker in the feed and the cross-linking density determined from the NMR analysis. Both the pull-off force and the elastic modulus are highly sensitive to the content of cross-linker but in opposite fashions. The reduced Young's modulus of the samples experienced a dramatic increase with increase at low cross-linker concentrations up to 3 wt % (MBA/AAc) or 0.01 mol fraction of MBA; afterward, it leveled off to a higher plateau. On the contrary, the adhesive pull-off force decreased drastically with increasing cross-linker concentration until 8 wt % (MBA/AAc) or 0.025 mol fraction of MBA in the hydrogel after which it reached a value close to zero. Hence, to obtain a poly(AAc-*co*-MBA) hydrogel film possessing good adhesive and mechanical properties, the degree of cross-linking should be kept within a MBA mol fraction range of 0.01−0.25; an optimal "trade-off" cross-linking density can be estimated as 0.02 mol fraction of MBA where balanced elastic modulus and adhesive force can be obtained.

Finally, it is worthwhile to discuss the relationship between the surface adhesion and bulk elasticity of the hydrogel films. There are two mechanisms contributed in the adhesion between two materials. The first mechanism refers to the interfacial interactions of two surfaces in contact, including covalent bonding, hydrogen bonding, and hydrophobic interactions. In addition, possible interdigitation and interpenetration of the outermost un-cross-linked polymer dangling chains can significantly affect the adhesion.[47] The second mechanism is related to the bulk deformation of the contacting materials, that is, the amount of energy dissipated during the separation. In our study, similar to other works in the literature, we most likely have some extent of interdigitation of the un-cross-linked polymer chains to the counter substrate[47] at low cross-linking density. Although poly(AAc-*co*-MBA) hydrogels

dx.doi.org/10.1021/jp3101688 | J. Phys. Chem. B 2013, 117, 441−449

are rich in −COOH moieties, the inert and hydrophobic nature of the PDMS tip limit the extent of interfacial interactions. In a separate study by Park and Robinson,[5] the mucoadhesion of a quite similar hydrogel is also attributed to the flexibility of the hydrogel chains and not the content of the −COOH groups on the surface. The counter substrate used in their study was more prone to interact with the hydrogels on the surface compared with our counter substrate. Therefore, it seems rational to attribute the observed adhesive pull-off force to the extent of mobility and flexibility of the chains in both gel bulk and the surface, which decreased with increasing cross-linking density. This might be the reason for the opposite effects of the cross-linking density on the adhesive pull-off force and the elastic modulus of PAA hydrogel films.

CONCLUSIONS

In summary, we reported a novel way to fabricate adhesive hydrogel films by photo polymerization of acrylic acid (AAc) with *N*,*N*′-methylenebisacrylamide (MBA) as a cross-linker in confined conditions and a detailed study of the effect of cross-linking on the properties of the hydrogel films. NMR spectroscopy has been utilized to determine the cross-linking density. We found that the cross-linking density determined by NMR is higher than that expected from the feed concentrations of cross-links, suggesting the heterogeneous nature of the cross-linking and that MBA is more reactive than AAc. The swelling tests and indentation tests were performed on the hydrogel films under water. As the feed cross-linker concentration C_{feed} increased, the degree of swelling remarkably decreased from 4000 to 500% when C_{feed} < 10 wt %. When C_{feed} > 10 wt %, the hydrogel films became opaque and the degree of swelling became constant; however, the opaqueness of the hydrogel films increased with C_{feed}, indicating a denser hydrogel network or higher degree of cross-links creating more pores but having smaller pore size. Effects of the cross-linker concentration on the adhesion and mechanical properties of the hydrogel films were systematically studied in terms of adhesive pull-off force and Hertz-type elastic modulus obtained by microindentation tests. As the cross-linker concentration increases, the effective elastic modulus of the hydrogel increases dramatically due to the increase in the number density of the cross-links until 0.01 mol fraction of MBA, after which it reaches a high steady−steady value. The adhesive pull-off force decreases with increasing cross-linker concentration until 0.025 mol fraction of MBA after which it reached a lower force plateau. An optimal "trade-off" cross-linking density was determined to be 0.02 mol fraction of MBA, where balanced elastic modulus and adhesive pull-off force can be obtained.

AUTHOR INFORMATION

Corresponding Author

*E-mail: zhaob@uwaterloo.ca.

Notes

The authors declare no competing financial interest.

ACKNOWLEDGMENTS

The authors would like to thank the Natural Sciences and Engineering Research Council of Canada (NSERC), Ontario Centre of Excellences (OCE), and Take Control Cosmedix Inc. for the financial support.

REFERENCES

(1) Peppas, N. A.; Mikos, A. G. Preparation Methods and Structure of Hydrogels. In *Hydrogels in Medicine and Pharmacy*; Peppas, N. A., Ed.; CRC Press: Boca Raton, FL, 1986.
(2) Park, K.; Shalaby, W. C. W.; Park, H. *Biodegradable Hydrogels for Drug Delivery*; Technomic: Lancaster, PA, 1993.
(3) Lorenz, D. H. U.S. Patent 5306504, 1992.
(4) Onuki, Y.; Hoshi, M.; Okabe, H.; Fujikawa, M.; Morishita, M.; Takayama, K. *J. Controlled Release* **2005**, *108*, 331−340.
(5) Park, H.; Robinson, J. R. *Pharm. Res.* **1987**, *4*, 457−464.
(6) De vries, M. E.; Bodde, H. E.; Busscher, H. J.; Hunginger, H. E. *J. Biomed. Mater. Res.* **1988**, *22*, 1023−1032.
(7) Drury, J. L.; Mooney, D. J. *Biomaterials* **2003**, *24*, 4337−4351.
(8) Khademhosseini, A.; Langer, R. *Biomaterials* **2007**, *28*, 5087−5092.
(9) Shull, K. *Mater. Sci. Eng., R* **2002**, *36*, 1−45.
(10) Bait, N.; Grassl, B.; Derailc, C.; Benaboura, A. *Soft Matter* **2011**, *7*, 2025−2032.
(11) Peppas, N. A.; Sahlin, J. J. *Biomaterials* **1996**, *17*, 1553−1561.
(12) Hoffman, A. *Adv. Drug Delivery Rev.* **2002**, *54*, 3−12.
(13) Stile, R. A.; Healy, K. E. *Biomacromolecules* **2002**, *3*, 591−600.
(14) Onuki, M.; Nishikawa, M.; Morishita, M.; Takayama, K. *Int. J. Pharm.* **2008**, *349*, 47−52.
(15) Sharma, A.; Jana, T.; Kesavamoorthy, R.; Shi, L.; Virji, M. A.; Finegold, D.; Asher, S. A. *J. Am. Chem. Soc.* **2004**, *126*, 2971−2977.
(16) Gudeman, L. F.; Peppas, N. A. *J. Membr. Sci.* **1995**, *107*, 239−248.
(17) Arndt, K.-F.; Richter, A.; Ludwig, S.; Zimmermann, J.; Kressler, J.; Adler, H.-J. *Acta Polym.* **1999**, *50*, 383.
(18) Park, S.-E.; Nho, Y.-C.; Kim, Y.-I. *Radiat. Phys. Chem.* **2004**, *69*, 221−227.
(19) Elliot, J. E.; Macdonald, M.; Nie, J.; Bowman, C. N. *Polymer* **2004**, *45*, 1503−1510.
(20) Myung, D.; Koh, W.; Ko, J.; Hu, Y.; Carrasco, M.; Noolandi, J.; Ta, C. N.; Frank, C. *Polymer* **2007**, *48*, 5376−5387.
(21) Marra, S. P.; Ramesh, K. T.; Douglas, A. S. *Mater. Sci. Eng., C* **2001**, *14*, 25−34.
(22) Zhao, X.; Huebsch, N.; Mooney, D. J.; Suo, Z. *J. Appl. Phys.* **2010**, *107*, 063509-(1−5).
(23) Stammen, J. A.; Williams, S.; Ku, D. N.; Guldberg, R. E. *Biomaterials* **2001**, *22*, 799−806.
(24) Baker, B. A.; Murff, R. L.; Milam, V. T. *Polymer* **2010**, *51*, 2207−2214.
(25) Calvet, D.; Wong, J. Y.; Giasson, S. *Macromolecules* **2004**, *37*, 7762−7771.
(26) Hu, Y.; Zhao, X.; Vlassak, J. J.; Suo, Z. *Appl. Phys. Lett.* **2010**, *96*, 121904-(1−3).
(27) Ebenstein, D. *Nano Today* **2006**, *1*, 26−33.
(28) Chan, E. P.; Hu, Y.; Johnson, P. M.; Suo, Z.; Stafford, C. M. *Soft Matter* **2012**, *8*, 1492−1498.
(29) Lin, D. C.; Shreiber, D. I.; Dimitriadis, E. K; Horkay, F. *Biomech. Model. Mechanobiol.* **2009**, *8*, 345−358.
(30) Constantinides, G.; Kalcioglu, Z. I.; McFarland, M.; Smith, J. F.; Van Vliet, K. J. *J. Biomech.* **2008**, *41*, 3285−3289.
(31) Jacot, J.; Dianis, S.; Schnall, J. *J. Biomed. Mater. Res., Part A* **2006**, *79*, 485−494.
(32) Lin, D. C.; Horkay, F. *Soft Matter* **2008**, *4*, 669−682.
(33) Lee, S. J.; Bourne, G. R.; Chen, X.; Sawyer, W. G.; Sarntinoranont, M. *Acta Biomater.* **2008**, *4*, 1560−1568.
(34) Arunbabu, D.; Sannigrahi, A.; Jana, T. *Soft Matter* **2011**, *7*, 2592−2599.
(35) Flory, P. J. *Principles of polymer chemistry*; Cornell University Press: Ithaca, NY, 1953.
(36) Mafe, S.; Manzanares, J. A.; English, A. E.; Tanaka, T. *Phys. Rev. Lett.* **1997**, *79*, 3086−3089.
(37) Lee, K.; Asher, S. A. *J. Am. Chem. Soc.* **2000**, *122*, 9534−9537.
(38) Baigl, D.; Seery, T. A. P.; Williams, C. E. *Macromolecules* **2002**, *35*, 2318−2326.

(39) Arunbabu, D.; Sanga, Z.; Seenimeera, K. M.; Jana, T. *Polym. Int.* **2009**, *58*, 88.
(40) Thevenot, C.; Khoukh, A.; Reynaud, S.; Desbrieres, J.; Grassl, B. *Soft Matter* **2007**, *3*, 437−447.
(41) Kemp, W. *Organic Spectroscopy*, 3rd ed.; Macmillan Education: London, 1991.
(42) Bovey, F. A.; Mirau, P. A. *NMR Spectroscopy of Polymers*; Academic press: San Diego, CA, 1996.
(43) Mowery, C.; Crosby, A.; Ahn, D. *Langmuir* **1997**, *7463*, 6101−6107.
(44) Stile, R.; Shull, K. *Langmuir* **2003**, *17*, 1853−1860.
(45) Gupta, R.; Frechette, J. Measurement and scaling of hydrodynamic interactions in the presence of draining channels. *Langmuir* **2012**, *28*, 14703−14712.
(46) Mattice, J. M.; Lau, A. G.; Oyen, M. L.; Kent, R. W. *J. Mater. Res.* **2006**, *21*, 2003−2010.
(47) Phadke, A.; Zhang, C.; Arman, B.; Hsu, C.-C.; Mashelkar, R. A.; Lele, A. K.; Tauber, M. J.; Arya, G.; Varghese, S. *Proc. Natl. Acad. Sci. U.S.A.* **2012**, *109*, 4383−4388.